Proceedings of International Collaboration on Advanced Neutron Sources (ICANS-VII), 1983 September 13-16
Atomic Energy of Canada Limited, Report AECL-8488

PRODUCTION RATES OF SPALLATION AND FISSION PRODUCTS IN DEPLETED URANIUM AND NATURAL LEAD TARGETS BOMBARDED BY 600 MeV AND 1100 MeV PROTONS

W.AMIAN* , N.F.PEEK**, D.J.SHADOAN**, G.STERZENBACH*

* Institut fuer Reaktorentwicklung
Kernforschungsanlage Juelich GmbH
Postfach 1913
D-5170 Juelich, Germany

** University of California at Davis
Physics Department
Davis, California 95616
U.S.A.

ABSTRACT

Reaction rates for fission products and spallation products produced by bombarding natural lead and depleted uranium foils with protons at 600 MeV and 1100 MeV have been determined using Ge(Li) spectroscopy methods. The foils were placed on the beam entrance face of a thick rectangular target block of the respective material. Spectra of gamma-rays emitted in the decay of these products between one hour and one year after irradiation were obtained. Gamma-rays were assigned to the responsible products by matching gamma-ray energies and half-lives. Reaction rates were then obtained from the data by first determining the appropriate gamma-ray activity as of the end of the irradiation, correcting for detector efficiency and gamma-ray transition probability and dividing by the beam current.
The resulting reaction rates are compared with model calculations at 1100 MeV. The general shapes of the distributions of reaction rates versus mass number agree fairly, but there are large discrepancies between individual data points and calculation. Reasons for this are discussed, especially regarding the effect of neutrons and secondaries which are produced in the target block.

INTRODUCTION

Lead and uranium are possible target materials for the German high flux neutron source SNQ. Therefore, it is required to study the production of residual activity in these target materials both from safety and maintenance aspects.

There are two possible ways to accomplish this task. The first is to study a nearly realistic spallation target in a mock-up experiment, map the induced activities at various positions inside the target and derive reaction rates at these points. This procedure has been adopted in the beginning of the SNQ study. It is, however, not possible to separate the combined influences of primary protons, secondary charged particles and fast or moderated neutrons. Thus, it is not straightforward to scale up the results to a real spallation target like the proposed target wheel.

Therefore, the second procedure, to study the fundamental high energy processes and to compare these results with model calculations, should be prefered. In this way, low energy neutron reactions, which are subject to normal reactor calculations, can be separated from high energy processes, and models for high energy spallation and fission processes can be compared with experimental data directely. This results in a combined effort to improve both the data basis and the model.

The present paper, actually, is between both procedures. Data which have been taken in connection with "infinitely thick" spallation targets have been reduced to obtain distributions of reaction rates as a function of mass number, so-called mass-yield distributions.
These have been compared with calculations for thin targets, although the influence of secondaries and neutrons could not be excluded.
The data for fission products and spallation products have been obtained in this study by gamma-ray assay of unseparated products in thin foils of uranium or lead. These foils have been bombarded by protons at 600 MeV and 1100 MeV and gamma-ray spectra have been recorded in time to follow the decay of individual gamma-ray lines.

EXPERIMENTAL

Target foils of 1.0 mm thickness and 30 mm diameter were placed on the beam entrance face of a large target simulating an "infinitely thick" spallation target. Two target materials were chosen for investigation, lead of natural composition and depleted uranium with an U-235 content of less than 0.5 %.
The experiments were conducted at Saturne National Laboratory (LNS) within the Centre d'Etudes Nucleaires de Saclay at proton energies of 600 MeV and 1100 MeV. The average beam intensity was up to 80 nA for the 1100 MeV runs and up to 25 nA for the 600 MeV runs. A more detailed description of the LNS experiments is given in reference /1/.
The uranium samples were vacuum encapsulated in aluminum cases to prevent the escaping of radioactive gases. Following each irradiation the samples were as quickly moved to the counting area as allowed by health physics considerations concerning the large target block. Short lived radioisotopes were out of the scope of this investigation.

A Ge(Li)-detector having an 80-cm^3 volume was used for the measurements. The output of the detector was amplified using standard equipment. The energy resolution for the 1332 keV line was 2.2 keV full-width at half-maximum. The detector was calibrated against IAEA and PTB standard reference sources with ±2% accuracy.
The samples were initially placed some meters from the face of the detector. When the counting rate had decreased, they were moved closer to the detector. Even at the closest distance of 23 cm, the detection efficiency is small enough to make true coincident gamma-ray summing negligible.

REACTION	cross section [mb]			REF.
	600 MeV	800 MeV	1100 MeV	
Al-27(p,3pn)Na-24	11.0+-3.3	10.5	9.9	[1]
	10.8+-0.7	10.5	10.2	[2]
		10.9+-0.2		[3]
		10.8		[6]
	11.0	10.75	10.4	[7]
Al-27(p,x)Na-22	19.6+-5.9	18	17	[1]
	13	12	11	[2]
	15	15.0+-1.5	15	[4]
		13.6		[6]
	17.3	16.3	14.8	[7]
Al-27(p,x)Be-7	4.0	5.4	7.0	[1]
	5	6.4+-0.6	8	[4]
			7.6	[5]
		5.7		[6]
	3.8	6.3	7.8	[7]
adopted values for beam monitor cross sections				
Al-27(p,3pn)Na-24	11.0	10.9+-0.2	10.5	
Al-27(p,x)Na-22	15.0		12.0	
Al-27(p,x)Be-7	5.0		7.6	

[1] G. FRIEDLANDER et al., Phys. Rev. 99(1955)263
based on a value of 10.8 mb for Na-24 at 450 MeV
as given by L.Marquez, Phys. Rev. 86(1952) 405
[2] J.B. CUMMING, Ann. Rev. Nucl. Sci. 13(1963)261
[3] J.B. CUMMING et al.,Nucl. Instr. Meth. 180(1981)37
[4] H.R. HEYDEGGER et al., Phys. Rev. C14(1976)1506
[5] E. BAKER et al., Phys. Rev. 112(1959)1319
[6] G. RUSSELL et al.,ICANS-V, Juelich 1981
[7] J.TOBAILEM et al., CEA-N-1466(1)

TABLE 1. Cross sections for aluminum monitor reactions from literature and adopted values for the present work. Values are interpolated if no error is stated.

The spectra were recorded in time, starting at best half an hour after end of irradiation. The last data were taken one year thereafter. Counting time intervalls ranged between five minutes and 24 houres.

The number of protons per second hitting the target was determined from monitor reactions in aluminum. Cross sections from literature and the adopted values for the reactions Al-27 (p,3pn) Na-24, Al-27 (p,x) Na-22 and AL-27 (p,x) Be-7 are given in table 1. The number of residual nuclei at end of irradiation is determined by gamma-ray spectrometric measurements. The adopted nuclear properties are given in table 2. From these measurements the beam intensities in table 3 follow.

ISOTOPE	HALFLIFE	GAMMA-RAY	
		ENERGY [KeV]	INTENSITY [%]
Be 7	53.4 d	477.56	10.3
Na 22	2.6 y	511.00	179.8
		1274.54	99.94
Na 24	15.03 h	1368.55	100.00
		2754.10	99.85

TABLE 2. Adopted decay properties of Na 24, Na 22 and Be 7.

TARGET MATERIAL	ENERGY [MeV]	INTENSITY [PROTONS/SEC]	DURATION [h]
LEAD	600	1.1E+11	0.53
LEAD	600	1.1E+11	0.66
LEAD	1100	4.3E+11	1.03
URANIUM	600	3.9E+10	0.58
URANIUM	1100	4.9E+11	0.95

TABLE 3. Beam intensities and irradiation times of the experiment discussed in the present paper.

As a reference cross section only the Al-27(p,3pn)Na-24 value was used which is given in the literature with more precision than the values for the other two reactions. For a beam intensity as calculated from a given Na 24 production the agreement between calculated cross sections for the other two reactions and the litrature values is only reasonable.
For the calculatons we assumed a 15% error in the beam intensities which results from counting error, error in taking the correct irradiation time and mainly the errors in production cross sections.
The irradiation times durated up to 62 minutes. The beam intensity was monitored in five minutes steps by a secondary emission chamber. All irradiations ran with only slightly varying beam current so that for the longer lived nuclides no corrections were necessary.
The gamma-ray spectra obtained were recorded on magnetic tape for subsequent computer analysis and isotope identification. They were first corrected for analyzer deadtime and for random summing effects. Then the peak areas were extracted using the computer code AGAMEMNON /2/. These results were input to the halflife analysis and nuclide identification code YELLOW /2/, which determines the gamma-ray intensities as a function of time following irradiation and assigns to the decay particular products based on matching the gamma-ray energies and nuclide halflives. The results were then corrected for decay during irradiation and for gamma-ray attenuation in the samples.

For the present data it was sufficient to include only one parent and one daughter decay, since most of the precurser nuclides have short lifetimes and had decayed completely by the initiation of the first measurement which revealed the respective nuclide. Details of the methods are reported in reference /2/.

The discussion shows that the reaction rates which to obtain is the final goal of the experiments are not the direct information of the applied experimental method. The primary experimental informations deduced from the measured spectra are photon activities of particular gamma-ray transitions from decay of fission and spallation products produced by the irradiation. To determine the reaction rate of a given product, both the knowledge of its nuclear properties and the knowledge of experimental parameters are required. Nuclear properties are gamma-ray transition probabilities and halflives of the product and its parent. Experimental parameters are detector efficiency at the respective energy, the irradiation history and the beam intensity as discussed above.
All these properties and parameters are themselves possible sources of errors. For non-fission products, especially in the lead region, even the nuclear properties are not so well known.
Thus, it should be evident, that mass-yield distributions derived from gamma-ray spectrometrical methods
- miss many mass chains, which have either weak gamma-ray emitters or no gamma-ray emitters at all,
- will only give results for a defined set of products with high reaction rates, strong gamma-ray intensities and long enough halflives, unless radiochemical separation methods are applied,
- show fluctuations even relative to each other due to different nuclear properties and their quite different influences in deriveing reaction rates from the decay characteristics of a specific gamma-ray transition.

RESULTS

The measured reaction rates for 48 fission and spallation products in natural lead are given in table 4; the data for 56 products in depleted uranium in table 5. Uncertainties include statistical errors, fitting errors from the decomposition of a gamma-ray line as a doublet or triplet, counting rate associated uncertainties, errors in the detector efficiency calibration and the uncertainty in beam intensity. They do not include any errors in nuclear properties of the respective fission or spallation products. Therefore, the nuclear properties adopted for the calculations are also tabulated in tables 4 and 5.
Most of them were obtained from the Erdtmann and Soyka compilation /3/ of gamma-ray lines and have been checked for consistency with the Lederer and Shirley compilation /4/. For the shorter lived products errors in halflives would contribute considerably to the errors given for the reaction rates. Uncertainties in the absolute gamma-ray intensities should be considered for all products.

Reaction rates for fission and spallation products were obtained primarily for nuclides having halflives greater than about one day and having reaction rates greater than 2E-07 reactions per proton per g/cm^2 in lead , and greater than 1E-06 reactions per proton per g/cm^2 in uranium. Reaction rates were not obtained for all nuclides within this defined set, particularly not for those that decay almost entirely by beta-ray emisssion, but also for a few for which the primary gamma-ray had nearly the same gamma-ray energy as a more intense gamma-ray from another nuclide having a similar halflife.

There were gamma-rays observed for which reaction rates were not obtained, even though the gamma-ray could have been ascribed to the decay of a specific product. In these cases the assignments were not almost certain.
We were satisfied with analyzing one or two gamma-rays associated with the decay of a given product, usually but not always the gamma-ray with the highest intensity.

We attempted to obtain information for additional products, particularly for the light mass products Fe, Cu, Zn, Ga, which are of importance in corrosion studies /5/.
Even when observed, however, the extracted reaction rates for the expected gamma-rays were not adequate to determine unambigously correct assignments. In our opinion, this can be accomplished only if radiochemical separation methods are applied.
For some products which have been observed in the 1100 MeV experiments no results are given at 600 MeV. There are two reasons for that. Firstly, the 600 MeV experiments have been conducted at lower beam currents. This is especially true for the uranium experiment. As a consequence, almost exclusively fission products have been observed. Secondly, for these runs the decay in time could not be recorded as needed due to technical problems (sharing the multichannel analyzer with another group, delay in shipping the foils from France to our laboratory).

NUCLIDE	GAMMA ENERGY /keV/	GAMMA INTENSITY / % /	HALFLIFE	HALFLIFE OF PARENT NUCLIDE	REACTION RATE 1E-6 react./proton/(g/cm**2) @ 1100 MeV	@ 600 MeV
67 Ho 160	728.10	61.00	25.0 m	1.19 d	15.1 +- 4.3	n.d.
69 Tm 165	242.90	35.10	1.253d	10.5 m	32.4 +- 5.4	n.d.
	296.08	23.11				
69 Tm 166	2052.90	20.15	7.7 h	2.363d	32.8 +- 8.2	n.d.
	778.80	19.82				
69 Tm 167	207.80	42.00	9.25 d	17.7 m	45.6 +- 7.1	n.d.
70 Yb 169	197.97	36.00	30.70 d	1.417d	48.4 +- 8.4	14.3 +- 3.2
	177.18	22.00				
	130.51	11.50				
71 Lu 170	1054.28	4.614	2.02 d	16.0 h	78.4 +- 20.3	n.d.
71 Lu 171	739.82	52.77	8.22 d	12.09 h	51.6 +- 10.6	12.7 +- 2.6
	667.60	11.64				
71 Lu 173	272.01	12.50	1.37 y	23.6 h	101 +- 17.5	31.1 +- 6.7
72 Hf 175	343.40	86.92	70.0 d	10.5 h	68.7 +- 17.1	22.9 +- 5.0
	432.80	1.56				
75 Re 183	162.32	24.97	70.4 d	13.0 h	65.2 +- 9.5	59.2 +- 12.7
76 Os 185	646.11	81.00	94.0 d	14 h	73.9 +- 10.4	72.6 +- 15.8
	880.27	5.152				
77 Ir 188	155.03	33.40	1.73 d	10.3 d	85.1 +- 15.8	73.0 +- 20.3
	633.10	21.60				
	1210.00	6.75				
	2012.00	0.50				
78 Pt 191	538.87	13.40	2.8 d	3.2 h	107 +- 14.9	147 +- 26.0
	359.88	5.89				
79 Au 195	98.86	11.80	183 d	9.5 h	86.0 +- 12.7	118 +- 25.5
81 Tl 200	367.97	88.4	1.088d	21.5 h	86.0 +- 12.5	73.9 +- 14.9
	579.28	14.0				
	828.32	11.0				
81 Tl 201	135.34	3.70	3.063d	9.4 h	121 +- 24.6	115 +- 18.6
82 Pb 203	279.18	80.80	2.171d	11.76 h	129 +- 20.7	101 +- 18.4
	401.31	3.80				
83 Bi 204	899.15	99.0	11.3 h	3.52 h	14.5 +- 1.9	17.7 +- 3.2
	374.74	75.0				
83 Bi 205	703.30	28.0	15.31 d	1.8 h	19.7 +- 4.1	n.d.
	1764.27	27.0				
	987.80	17.0				
83 Bi 206	803.05	100.00	6.243d	8.83 d	9.9 +- 1.3	n.d.
	881.00	67.60				
	1718.65	34.00				
83 Bi 207	569.67	98.0	38 y	5.8 h	10.6 +- 1.7	9.7 +- 2.2
25 Mn 52	1434.30	100.00	5.7 d	8.3 h	0.71 +- 0.15	n.d.
25 Mn 54	834.81	99.978	312.2 d		0.95 +- 0.13	0.43 +- 0.11
30 Zn 65	1115.52	50.75	243.8 d	15.2 m	2.4 +- 0.2	n.d.
34 Se 75	264.65	58.60	120.4 d	1.63 h	3.7 +- 0.4	1.5 +- 0.4
	279.53	24.73				
	400.65	11.13				
37 Rb 83	529.54	30.0	86.2 d	32.4 h	5.8 +- 0.7	5.2 +- 1.1
	552.50	16.3				
38 Sr 85	513.99	99.28	64.73 d	2.7 h	6.1 +- 1.1	5.4 +- 1.1
39 Y 87	484.72	92.2	3.346d	1.6 h	6.5 +- 1.1	n.d.
39 Y 88	1836.01	99.36	106.6 d	83.4 d	8.4 +- 1.7	9.5 +- 2.2
	898.02	94.00				
40 Zr 89	909.20	99.87	3.268d	2.02 h	4.8 +- 0.7	n.d.
45 Rh 101m	306.77	86.7	4.34 d	8.5 h	8.2 +- 1.1	n.d.
45 Rh 102	475.00	93.00	2.89 y		3.0 +- 0.4	2.4 +- 0.7
	631.10	55.80				
	697.10	44.64				
47 Ag 105	344.20	40.9	41.3 d	56.0 m	3.5 +- 0.7	19.9 +- 4.5
	280.30	29.7				
	644.55	10.2				
	443.37	10.8				
50 Sn 113	391.71	64.17	115.1 d	6.74 m	0.2 +- 0.04	n.d.
	255.04	2.07				
52 Te 121	573.08	79.10	16.8 d	2.12 h	1.7 +- 0.2	1.5 +- 0.4
58 Ce 139	165.85	80.0	137.5 d	4.5 h	2.2 +- 0.2	n.d.
61 Pm 143	742.00	38.50	265 d	8.83 m	2.6 +- 0.4	n.d.
63 Eu 146	747.13	98.60	4.6 d	48.3 d	1.1 +- 0.2	0.43 +- 0.17
	1408.80	3.30				
63 Eu 149	327.70	3.8	93.1 d	9.4 d	10.8 +- 3.5	n.d.
21 Sc 46	1120.52	99.99	83.85 d		0.50 +- 0.15	n.d.
21 Sc 48	1311.80	99.99	1.825d		0.60 +- 0.15	n.d.
26 Fe 59	1099.22	56.50	45.1 d		1.7 +- 0.2	n.d.
	1291.56	43.20				
40 Zr 95	724.18	44.20	64.4 d	10.3 m	4.1 +- 0.4	3.9 +- 0.9
	756.72	54.80				
44 Ru 103	497.08	86.40	39.35 d	50 s	7.1 +- 1.5	8.0 +- 1.7
	610.33	5.30				
45 Rh 106	621.80	9.806	29.9 s	368.2 d	2.2 +- 0.4	n.d.
	1050.10	1.463				
47 Ag 110m	657.72	94.74	249.9 d		1.9 +- 0.4	2.6 +- 0.7
	884.67	72.86				
65 Tb 160	876.37	30.0	72.1 d		13.4 +- 3.2	22.3 +- 4.8
	966.17	25.5				
80 Hg 203	279.17	81.50	46.59 d		11.7 +- 1.1	15.1 +- 3.2

TABLE 4. Reaction rates of spallation and fission products produced by protons of 1100 MeV and 600 MeV at the beam entrance surface of a thick rectangular target of natural lead. The data are ordered by mass numbers in three groups each. The first group consists of spallation products, the second of neutron deficient high energy fission products, the third of neutron rich fission products and othar β^- emitters.

NUCLIDE	GAMMA ENERGY /keV/	GAMMA INTENSITY / % /	HALFLIFE	HALFLIFE OF PARENT NUCLIDE	REACTION RATE 1E-5 react./proton/(g/cm**2) @ 1100 MeV	REACTION RATE 1E-5 react./proton/(g/cm**2) @ 600 MeV
26 Fe 59	1099.22	56.50	45.1 D		0.73 +- 0.05	n.d.
	1291.56	43.20				
36 Kr 87	402.70	48.3	76.4 m	55.6 s	7.4 +- 0.9	n.d.
39 Sr 91	555.57	60.7	9.67 h	58 s	12.2 +- 1.1	n.d.
40 Zr 95	724.18	44.20	64.4 d	10.3 m	23.8 +- 2.2	17.5 +- 2.6
	756.72	54.80				
40 Zr 97	743.36	98.00	16.8 h	3.7 s	19.3 +- 2.2	20.5 +- 3.5
42 Mo 99	140.51	90.90	2.758d	2.6 m	17.7 +- 2.3	21.6 +- 3.6
44 Ru 103	497.08	86.40	39.35 d	50 s	32.4 +- 3.0	31.9 +- 5.3
	610.33	5.30				
45 Rh 105	319.24	19.6	1.473d	4.44 h	22.9 +- 2.1	19.1 +- 3.6
	306.31	5.44				
45 Rh 106	621.80	9.806	29.9 s	368.2 d	15.6 +- 1.5	15.4 +- 2.4
	1050.10	1.463				
47 Ag 112	1387.00	5.4	3.14 h	21.1 h	13.3 +- 4.8	10.3 +- 1.2
	616.80	43.5				
48 Cd 115	336.30	46.10	2.224d	20.0 m	7.6 +- 0.7	9.0 +- 1.6
	527.86	32.90				
	492.29	10.20				
51 Sb 125	427.95	29.60	2.77 y	9.64 d	6.3 +- 0.5	5.4 +- 0.9
	636.15	11.20				
	463.51	10.00				
51 Sb 127	685.50	35.7	3.85 d	2.1 h	6.2 +- 0.7	n.d.
	473.00	25.0				
	783.80	15.0				
52 Te 129	459.50	7.14	1.16 h	4.32 h	3.4 +- 0.4	2.9 +- 0.5
52 Te 132	116.30	1.95	3.246d	4.1 m	16.9 +- 1.8	13.6 +- 2.3
	228.16	88.50				
53 J 134	884.08	66.00	52.6 m	41.8 m	23.6 +- 4.3	n.d.
	847.03	96.00				
55 Cs 137	661.62	84.62	30.1 y	3.92 m	18.7 +- 1.8	17.6 +- 2.0
56 Ba 139	165.80	18.8	1.415h	9.3 m	18.8 +- 2.5	16.9 +- 2.8
57 La 140	1596.20	95.47	40.27 h	12.79 d	17.7 +- 1.4	17.4 +- 2.8
	815.80	22.32				
	487.03	43.00				
58 Ce 141	145.45	48.00	32.38 d	3.93 h	14.6 +- 2.1	9.4 +- 2.6
57 La 142	641.17	52.50	1.542h	10.7 m	11.9 +- 1.2	n.d.
58 Ce 143	293.30	43.4	33.7 h	14.0 m	10.6 +- 1.0	10.5 +- 1.8
58 Ce 144	133.53	10.8	284.2 d	39.8 s	11.9 +- 1.6	10.9 +- 1.9
60 Nd 147	531.00	13.5	11.06 d	12 m	7.6 +- 0.7	5.0 +- 1.1
63 Eu 156	2026.61	3.502	15.19 d	9.4 h	0.53 +- 0.2	n.d.
30 Zn 65	1115.52	50.75	243.8 d	15.2 m	0.25 +- 0.03	n.d.
31 Ga 68	1077.44	3.30	1.13 h	287 d	0.48 +- 0.15	n.d.
34 Se 75	264.65	58.60	120.4 d	1.63 h	0.51 +- 0.10	n.d.
	279.53	24.73				
	400.65	11.13				
37 Rb 83	529.54	30.0	86.2 d	32.4 h	1.4 +- 0.1	n.d.
	552.50	16.3				
39 Y 87	484.72	92.2	3.346d	1.6 h	0.73 +- 0.08	n.d.
39 Y 88	1836.01	99.36	106.6 d	83.4 d	2.1 +- 0.2	1.2 +- 0.4
	898.02	94.00				
40 Zr 89	909.20	99.87	3.268d	2.02 h	0.61 +- 0.08	n.d.
41 Nb 91m	1205.00	3.4	64 d	15.49 m	1.3 +- 0.3	n.d.
45 Rh 101m	306.77	86.7	4.34 d	8.5 h	1.3 +- 0.1	n.d.
47 Ag 105	344.20	40.9	41.3 d	56.0 m	1.3 +- 0.2	n.d.
	280.30	29.7				
	644.55	10.2				
	443.37	10.8				
50 Sn 113	391.71	64.17	115.1 d	6.74 m	0.89 +- 0.10	n.d.
	255.04	2.07				
52 Te 121	573.08	79.10	16.8 d	154 d	1.5 +- 0.2	n.d.
54 Xe 127	202.84	68.0	36.41 d	6.25 h	2.7 +- 0.3	1.9 +- 0.7
	172.10	25.4				
	374.96	17.7				
58 Ce 139	165.85	80.0	137.5 d	4.5 h	1.6 +- 0.2	n.d.
61 Pm 143	742.00	38.50	265 d	8.83 m	1.2 +- 0.1	n.d.
63 Eu 146	747.13	98.60	4.6 d	48.3 d	0.11 +- 0.01	n.d.
	1408.80	3.30				
79 Au 192	316.50	84.75	4.1 h	4.9 h	3.8 +- 0.3	n.d.
	295.98	32.63				
79 Au 194	328.50	60.90	1.646d	260 y	4.1 +- 0.4	n.d.
	293.60	10.663				
81 Tl 200	367.97	88.4	1.088d	21.5 h	3.8 +- 0.8	n.d.
	579.28	14.0				
	828.32	11.0				
83 Bi 204	899.15	99.0	11.3 h	3.52 h	3.6 +- 1.2	n.d.
	374.74	75.0				
83 Bi 205	703.30	28.0	15.31 d	1.8 h	1.8 +- 0.2	n.d.
	1764.27	27.0				
	987.80	17.0				
83 Bi 206	803.05	100.00	6.243d	8.83 d	1.9 +- 0.2	n.d.
	881.00	67.60				
	1718.65	34.00				
83 Bi 207	569.67	98.0	38 y	5.8 h	6.0 +- 0.7	n.d.
85 At 209	782.00	58.0	5.42 h	30 m	2.6 +- 0.3	2.0 +- 0.4
	792.00	37.0				

TABLE 5. continued on next page

NUCLIDE	GAMMA ENERGY /keV/	GAMMA INTENSITY / % /	HALFLIFE	HALFLIFE OF PARENT NUCLIDE	REACTION RATE 1E-5 react./proton/(g/cm**2) @ 1100 MeV	REACTION RATE @ 600 MeV
86 Rn 211	947.20	27.0	14.60 h	3.1 m	2.3 +- 0.3	3.3 +- 0.6
	1135.00	18.0				
	250.10	10.0				
91 Pa 230	951.95	28.09	17.4 d		1.0 +- 0.1	1.3 +- 0.2
	918.50	7.95				
	898.65	5.618				
91 Pa 232	969.30	41.62	1.31 d		1.8 +- 0.3	2.3 +- 0.4
	894.30	19.84				
	150.10	10.84				
92 U 237	207.95	22.40	6.75 d	8.7 m	35.0 +- 8.6	63.5 +- 10.6
93 Np 239	277.60	14.10	2.355d	23.5 m	58.2 +- 5.6	59.5 +- 9.9
	228.19	10.72				

TABLE 5. Reaction rates of spallation and fission products produced by protons of 1100 MeV and 600 MeV at the beam entrance surface of a thick rectangular target of depleted uranium. The data are ordered by mass numbers in three groups each. The first group consists of neutron rich fission products, the second of neutron deficient high energy fission products, the third of spallation products.
(Continuation from previous page)

DISCUSSION

The primary purpose of this experiment was to measure reaction rates for fission and spallation products created during bombardement with high energy protons.
These reaction rates are plotted for the lead targets in figure 1 versus mass number of the residual nuclei both at 600 MeV and at 1100 MeV. All points are plotted with their experimental errors (one standard deviation). Arrows indicate that a stable reaction product is missing with certainty and, therefore, the total reaction rate of this mass chain is higher than indicated.

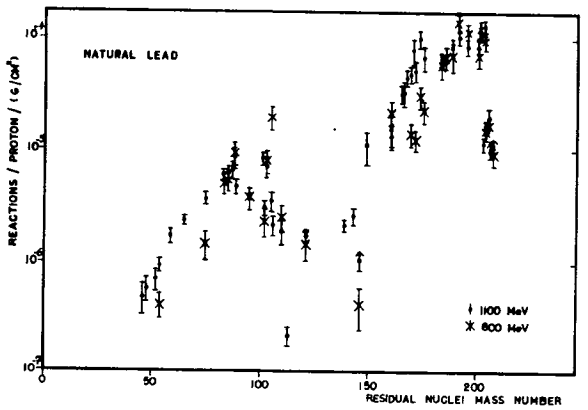

FIGURE 1 Distribution of reaction rates versus mass number for spallation and fission products produced by protons of 1100 MeV and 600 MeV, respectively, at the beam entrance surface of a thick rectangular target of natural lead.

The data for lead indicate that for mass numbers less than about 130 the reaction rates and, therefore, the shapes of the mass-yield distributions are nearly the same at 600 MeV and 1100 MeV. Also near to the mass numbers of the lead isotopes the reaction rates are nearly the same. In the intermediate region, however, there seems to be a difference in both shapes. While the 600 MeV data fall off steeply as mass number decreases (except for Ho 160, which is a β^- emitter), the 1100 MeV data seem to have a new maximum around 170 mass units and then the production rates fall off like at 600 MeV, with the location of the gradient shifted by about 10 mass units.

The 600 MeV results for uranium are compared in figure 2 to the 1100 MeV data. Because of the low beam intensity for this experiment, mainly fission products have been observed. It is not astonishing that their reaction rates agree well at 600 MeV and at 1100 MeV within the errors stated. Concerning the non-fission products with masses below 160 mass units there have been only two assignments which indicate that the reaction rates at 600 MeV are about one half the ones at 1100 MeV. There have been no assignments at 600 MeV for mass numbers between 160 and 208. Results for the higher mass numbers are similar within the experimental errors.

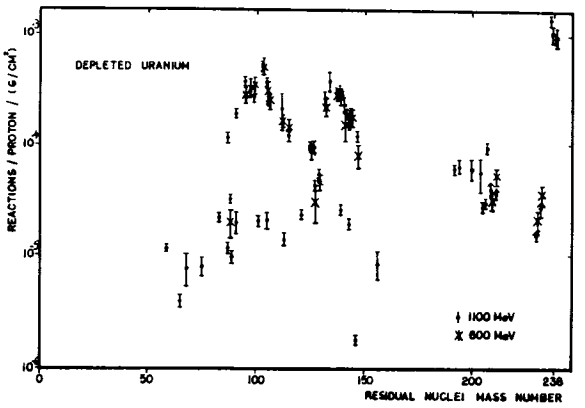

FIGURE 2 Distribution of reaction rates versus mass number for spallation and fission products produced by protons of 1100 MeV and 600 MeV, respectively, at the beam entrance surface of a thick rectangular target of depleted uranium.

The results shown in figures 1 and 2 are compared with HET calculations /6/ for 1100 MeV protons hitting lead targets, figure 3, and hitting uranium targets, figure 4. The calculations are for thin targets, i.e. no secondaries are considered to interact with a target nucleus. This situation is the easiest to calculate and gives only the residual nuclei left by high energy processes.
The calculated numbers of residual nuclei within a three mass unit interval are plotted as histograms in figures 3 and 4. The normalization is for a total inelastic cross section of 1.776 barns for the lead data and 1.983 barns for the uranium data. The errors from Poisson statistics of the calculated histogram are at worst 20%.

For natural lead, figure 3, calculation and experiment agree fairly only at the higher masses near to the masses of lead. At lower mass numbers it is evident that the calculated mass-yield distribution is shifted towards lower mass numbers by about 20 units. There is no obvious reason for that.
From the experimental point of view it is hard to imagine how a successive row of experimental points should be systematically too low by a factor of 4 while other points fit the calculation well. The only reason might be that we are missing stable nuclides and nuclides decaying from the opposite side towards the stability line. The influence of secondaries should go into the opposite direction.

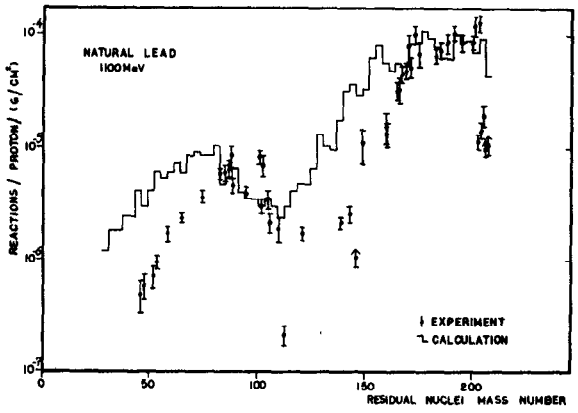

FIGURE 3 Comparison of experimental and calculated distributions of reaction rates versus mass number of, spallation and fission products produced by protons of 1100 MeV on lead. The calculations are done with HETC (JUEL-SPEZ-196) and apply to thin targets, whereas the measurements have been performed on the beam entrance surface of a thick rectangular target.

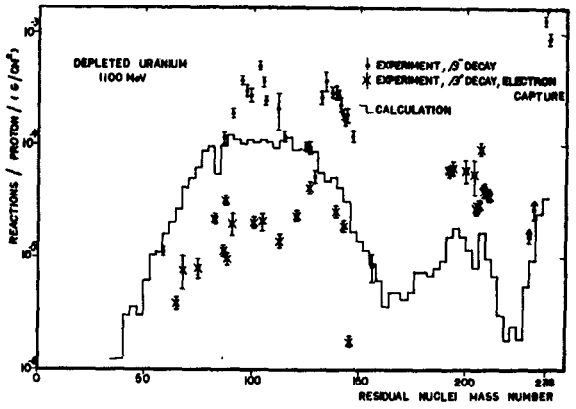

FIGURE 4 Comparison of experimental and calculated distributions of reaction rates versus mass number of spallation and fission products produced by protons of 1100 MeV on uranium. The calculations are done with HETC (JUEL-SPEZ-196) and apply to thin targets, whereas the measurements have been performed on the beam entrance surface of a thick rectangular target.

Turning to depleted uranium, figure 4, the agreement between experiment and calculation is bad again. In this figure we distinguish between nuclides which are β^- emitters and nuclides which decay by β^+ or electron capture. The β^- emitters between mass numbers 50 and 170 may be refered to as fission products. Their reaction rates are higher than anticipated from calculations for the thin target. The reason is that neutrons produced in the thick target initiate fissions in the thin target, too. Referring to the calculations, however, high energy fisson products from bombarding uranium with protons do not only consist of neutron deficient isotopes as indicated by the crosses in figure 4, but also include some "normal" fission products, i.e. neutron rich isotopes. Thus, the high energy fission process is completely hidden by fissions from neutrons of intermediate energy.

A remarkable fact is that the center of the calculated fission peak is shifted towards lower mass numbers relatively to the experimentally observed double fission peak by about 15 to 20 mass units.
The satellite peak at masses around 200 units is reproduced, but the experimental values are about half an order of magnitude higher. The same is true for the steep decrease below mass number 238. Not reproduced by the calculations are the reaction rates for U 237 and Np 239. The latter, however, is produced by neutrons and not by protons.

In conclusion, the experimental and calculated mass-yield distributions given for uranium and lead are far from being consistent. Both experiment and model may be in error. Especially for uranium, the comparison with a thin target experiment would be of great interest.

CONCLUSION

The goal of the present experiment was to deduce reaction rates of fission products and spallation products produced during irradiation of natural lead and depleted uranium with protons at 600 MeV and 1100 MeV.
Although the basic spectral data appear quite complicated, for most of the gamma-rays given in tables 4 and 5 data reduction was not unusually difficult. Experimental errors have been given which include statistical errors, fitting errors for the decomposition of a gamma-ray line as a doublet or triplet, counting rate associated uncertainties, error in detector efficiency and uncertainties in beam intensity.
The major weakness in determining reaction rates for fission and spallation products by this technique is the rely on nuclear data; such data have different influences on the various products and result in nonuniform scatter in the data. Errors of these nuclear data have not been included in the experimental errors given, because they are normally not tabulated in the compilations /3/,/4/.
It is apparent that the reaction rates given in tables 4 and 5 will change as nuclear data measurement become more accurate.

The comparisons of the present experimental data and model calculations with HETC /6/ do not give encouraging consistencies, although the genaral shape is similar. At small and intermediate mass numbers the calculated mass-yield distributions seem to be shifted by 15 to 25 mass units towards smaller masses. It has to be pointed out, however, that the calculations are made for thin targets, whereas the measurements have been performed on the surface of an "infinitely thick" spallation target.
To reduce the influence of secondaries and neutons, an experiment to measure the production rates of thin targets has been planned at 800 MeV proton energy.

REFERENCES

/1/ W.AMIAN, N.F.PEEK, D.J.SHADOAN, Gamma-Ray Measurements of Isotopes Produced by 1.1 GeV Protons on Lead and Uranium Targets, ICANS-V, Juelich 1981
/2/ W.AMIAN, N.F.PEEK, D.J.SHADOAN, Measurements of the Spallation and Fission Product Production for Depleted Uranium and Natural Lead Targets Bombarded by 1100 MeV Protons, ICANS-VI, Argonne 1982
/3/ G.ERDTMANN, W.SOYKA, The Gamma-Rays of the Radionuclides, Verlag Chemie, Weinheim and New York 1979
/4/ C.M.LEDERER, V.S.SHIRLEY, Tables of Isotopes,Seventh Edition, John Wiley & Sons, New York 1978
/5/ W.LOHMANN, A.RIBBENS, private communications
/6/ P.CLOTH, D.FILGES, G.STERZENBACH, T.W.ARMSTRONG, B.L.CALBORN, The KFA-Version of the High-Energy Transport Code HETC and the Generalized Evaluation Code SIMPEL, JUEL-SPEZ-196, March 1983